N86-26687

FLUIDIZED-BED REACTOR MODELING FOR PRODUCTION OF SILICON BY SILANE PYROLYSIS

M. P. Dudukovic̀, P. A. Ramachandran and S. Lai

Washington University
St. Louis, Missouri 63130, USA

INTRODUCTION

Traditionnally high purity silicon for solar and electronic applications has been produced in Siemens decomposers by hydrogen reduction of chlorosilanes [1]. The yield in the Siemens process is poor. The new cheap routes to silane offer an attractive alternative for silicon production via silane pyrolysis. The thermodynamic yield of this process is 100%. However, higher feed concentrations of silane (a few percent) in Siemens decomposers lead to formation of fines via homogeneous nucleation. In order to realize the potential of silane pyrolysis the formation of fines must be prevented or at least kept below a certain acceptable minimum level. Fluidized beds offer an attractive possibility, and extensive experimental studies have been conducted [2,3]. Modeling efforts have lagged far behind the experimental activities.

The objective of this paper is to develop a mathematical model for fluidized bed pyrolysis of silane that relates production rate and product silicon properties (such as size, size distribution, presence and absence of fines) with fluidized-bed size and operating parameters (such as wall temperature, feed concentration, gas flow rate, seed size, etc.) and with bed grid design. Upon model verification it is desired to expand the model to account for product morphology, i.e. porous versus nonporous particles, etc. While fluidized-bed models for catalytic processes are abundant (e.g. see reviews by Grace or Yates [4,5,6]) and models for gas-solid reactions with changing solids have been well established by Kunii and Levenspiel [7,8], a comprehensive model needed for simultaneous chemical vapor deposition (CVD) and nucleation reactions has not been reported.

MODEL DEVELOPMENT

A suitable mathematical model for silane pyrolysis in fluidized-bed reactors should consider various reaction pathways, the problem of "smoke" (fines) formation, the suppression of "smoke" formation and its capture by large particles. We approach these problems on two levels. First, we attempt to identify a plausible description of the key chemical and physical rate determining steps in reaction pathways from silane to silicon. Then we address the question of flow and gas-solid contacting in fluidized-beds, and develop a model for the reactor. We treat here only batch growth of solids because data are readily available only for this model of operation.

Reaction Pathways from Silane to Solid Silicon

The mechanism of silane pyrolysis is not completely understood [1]. Active

work is in progress in addressing this question [9,10]. We do not know for certain which intermediate species is the first to nucleate. Based on the current understanding of the system we arrive at the picture presented in Figure 1 for the various pathways from silane to silicon. We assign the rate of the rate limiting step to each pathway. In doing so we have assumed that silane can decompose by two independent pathways. One is the homogeneous decomposition (pathway 3) into a gaseous precursor that can nucleate a new solid phase of silicon. We use the form reported by Hogness et. al. [11] with the variations suggested by either Purnell and Walsh [12] or O'Neal and Ring [13] to describe it. The other route for silane decomposition is the heterogeneous chemical vapor decompostion (CVD) of silane on the existing silicon seed particles (pathway 1) or on the formed nuclei (pathway 2). For this rate we use the first-order form reported by Iya et. al. [14]. It can readily be shown that in fluidized beds, due to rapid particle-gas transfer, CVD would control the growth rate of large particles rather than mass transfer. Since the molecular bombardment rate of small particles (fines) is larger than the CVD rate at the temperature of interest (500 to 750°C) then CVD also controls the silane loss to fines (pathway 2).

The intermediate which leads to the nucleation of the new phase is assumed to be the silicon vapor. The concentration of this intermediate formed by homogeneous pathway 3 is always very small. By pathway 4 nucleation of critical size nuclei, r*, occurs whenever supersaturation S = 1 is exceeded. The concentration of silicon vapor can be suppressed by diffusion and condensation on large particles (pathway 6) and by molecular bombardment of fines (pathway 5). We assume here that nucleation occurs by the homogeneous nucleation theory [15]. The molecular bombardment rate of small particles (pathway 5) is calculated by the classical expression of kinetic theory [16] while the diffusion rate to large particles (pathway 6) is readily obtained from film theory of mass transfer [16]. This concludes the description of those pathways in Figure 1 that include gaseous and solid·species. The rate forms used are indicated on the figure.

Population Balance for Fines

In order to describe the size of fines and the ability of large particles to scavenge them, we need a population balance for fines. We define $n_v(v)dv$ to be the number of fines having volumes in the range v to v + dv per unit volume of the gas. The population balance, based on a well mixed gas volume, yields the following equation:

$$\frac{q_e}{V_I} n_v(v) + \frac{\partial}{\partial v} [R_G(v) \, n_v(v)] = \frac{1}{2} \int_{v*}^{v-v*} \beta(v-\tilde{v},\tilde{v}) \, n_v(v-\tilde{v}) \, n_v(\tilde{v}) d\tilde{v}$$

$$- \int_{v*}^{\infty} \beta(v,\tilde{v}) \, n_v(v) \, n_v(\tilde{v}) d\tilde{v} - \alpha(v,v_L) \, n_v(v) + r_{HN} N_A \, \delta(v-v*) \tag{1}$$

The LHS terms of Eq. (1) are the elutriation rate and growth rate into size range by CVD of silane and molecular bombardment of Si vapor. The RHS terms are growth rate into size range by coagulation of fines, rate of loss in size range by coagulation, rate of loss in size range by scavenging by large particles (seeds) and the nucleation rate of the critical size. The pseudo-state approximation is used here since we are interested in observing the system at the time
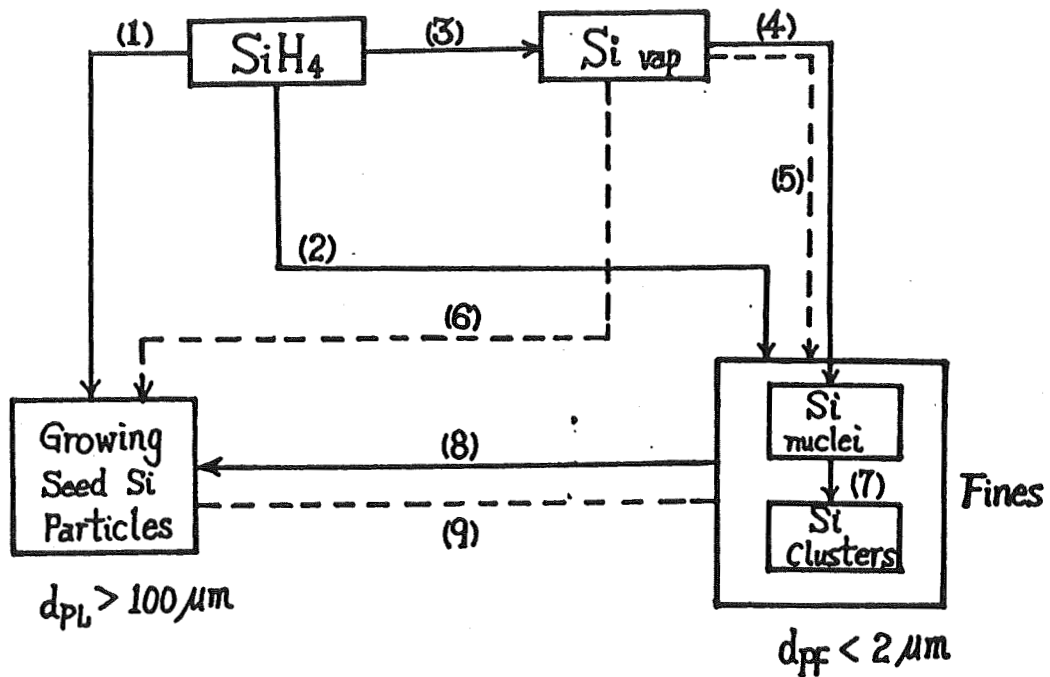
(1) CVD growth on seed particles $\Big\}$ $r_{HT} = 2.79 \times 10^8 \exp(-19530/T) \, C_{SiH_4}$

(2) CVD growth on fines $\quad$ Heterogeneous decomposition

(3) Homogeneous silane decomposition $\quad r_{HD} = 2 \times 10^{13} \exp(-26,000/T) \, C_{SiH_4}$

(4) Homogeneous nucleation $\quad r_{HN} = (N_A \dfrac{\alpha_c}{\rho_{Si}} (\dfrac{2\bar{\sigma}m}{\pi})^{1/2}) \exp(-\dfrac{4\pi r^*\bar{\sigma}N_A}{3R_gT}) \, C_{Si}*^2$

(5) Molecular bombardment of fines $\Big\}$ Si diffusion $\quad r_{DF} = \phi_s \sqrt{R_gT/2\pi M_{Si}} \, (C_{Si}-C_{Si_o})$

(6) Diffusion to growing seeds $\quad r_{DL} = (2\phi_s D/d_{PL}) \, (C_{Si}-C_{Si_o})$

(7) Coagulation and coalescence of fines — eq. (4)

(8) Scavenging by seed particles on fines — eq. (10)

(9) Attrition of large particles (not included)

Figure 1. Schematic of Various Pathways for Conversion of
Silane to Silicon.

scale for growth of large particles which is very long compared to other time scales.

It should be kept in mind that we are not interested in a precise description of the size distribution of fines. We mainly need to establish if their formation can be suppressed and if not, what their mean size might be. We, therefore, solve the population balance approximately by using the method of moments. We define:

$$M_0 = \int_{v*}^{\infty} n_v(v)dv = \text{(total number of particles per unit volume of gas)} \tag{2}$$

$$M_1 = \int_{v*}^{\infty} vn_v(v)dv = \text{(total volume of particles per unit volume of gas)} \tag{3}$$

The number average mean volume of fines is then obtained by the ratio of the first and zeroth moment $\bar{v} = M_1/M_0$. In order to reduce eq. (1) to a set of equations for the moments we need to make a set of assumptions. These are:

i) The coagulation coefficient is assumed to be a constant which only depends on the average size of fines. This approach is often used in the continuum regime where the problem is thus reduced to a Smoluchowski type equation [16,17]. We use the same approach for the free molecular regime and take the following value of the coagulation coefficient β_0

$$\beta_0 = \begin{cases} \dfrac{8kT}{3\mu} & \text{continuum region} \tag{4a} \\[2ex] 2^{5/2} (\dfrac{3}{4\pi})^{1/6} (\dfrac{6kT}{\rho_p}) \bar{v}^{1/6} & \text{free molecular regime} \tag{4b} \end{cases}$$

ii) The scavenging coefficient is assumed to be dependent only on the mean size (diameter) of the large seed particles and of the fines. Following the work of Doganoglu et. al. [18] and Peters et. al. [19] we represent the scavenging coefficient of fines by large particles in a fluidized bed by:

$$\alpha(\bar{v}_L, \bar{v}_F) = E\, u_{mf} \frac{3(1-\varepsilon_{mf})}{2\bar{d}_{PL}\, \varepsilon_{mf}} \tag{5}$$

where ε_{mf}, u_{mf} are bed voidage and superficial gas velocity at minimum fluidization, α is the scavenging coefficient, $\bar{d}_{PL}$ is the mean diameter of large particles (seeds) and E is the single large particle collection efficiency. It is well established [16,17] that single body collection efficiency can be approximately represented as a sum of efficiency for impaction, interception, diffusion, and diffusion with interception. The diffusional mechanism dominates under the conditions prevailing in a fluidized bed reactor and

$$E = 2\, Pe^{-2/3} \tag{6}$$

where $Pe = \bar{d}_{PL}\, u_{mf}/D$ and $D = kT/3\pi\mu\, \bar{d}_{PF}$. The mean particle diameter for small and large particles is estimated.

iii) The growth rate of fines, which is due to the combined effect of CVD growth from silane and molecular bombardment of gaseous silicon, is assumed to be given as a function of the average size of fines, i.e.

$$\int_{v^*}^{\infty} v \frac{\partial}{\partial v} [R_G(v)n_v(v)]dv = -\sigma \bar{v}^{-2/3} M_0 = -\sigma \bar{v}^{-1/3} M_1 = -\sigma M_0^{1/3} M_1^{2/3} \qquad (7)$$

where $\sigma = (M_{Si}/\phi_s \rho_{Si})(4)^{1/3} 3^{2/3}(r_{HT} + r_{DF})$.

With the above three assumptions the population balance, eq. (1), is reduced to the following two equations for the moments:

$$-\frac{1}{2} \beta_0 M_0 - (\alpha + \frac{q_e}{V_I}) M_0 - r_{HN}N_A = 0 \qquad (8)$$

$$\sigma M_0^{1/3} M_1^{2/3} - (\alpha + \frac{q_e}{V_I}) M_1 + r_{HN}N_A v^* = 0 \qquad (9)$$

The scavenging rate of fines by large particles is now given by:

$$m_{Sca} = \frac{Si}{N_L} \int_{v_L min}^{v_L max} \int_{v_F min}^{v_F max} v_F \alpha(v_L,v_F)n_L (v_L) n_F (v_F) dv_L dv_F \qquad (10)$$

with the scavenging coefficient α given by eq. (5).

This completes the description of various pathways of Figure 1, namely pathway 7, by which a population of fines with a certain average size is established, and of pathway 8 for scavenging (filtering) of fines by large particles.

Backmixed Reactor (CSTR) Model

The hydrodynamics of a fluidized bed and gas-particle contacting are complex and not entirely understood. It is useful, however, to develop models that characterize the limiting behavior of the system which can only be approached in practice. Here we deal with the competitive homogeneous and heterogeneous reaction. Intimate gas-solid contacting, high solids to gas ratio and no gas by-passing will favor the heterogeneous route. Homogeneous nucleation is to be prevented compared to CVD growth and diffusion of Si vapor. The former can be regarded as a reaction of high order and, hence, will be suppressed the most by complete micromixing such as found in an ideal CSTR. Therefore, both suppression of homogeneous decomposition and of homogeneous nucleation will be favored in a CSTR, i.e. in an ideally backmixed reactor. This situation can be approached in fluidized beds when bubble formation is suppressed while good solids mixing is maintained.

We formulated the CSTR model based on the following assumptions: i) no wall deposition, i.e. negligible wall to particles area, ii) no temperature gradients between the gas and particles, iii) uniform composition and temperature in the reactor. In addition, for the results presented in this paper, we assumed that all seed particles have the same initial size and grow at the same rate.

The equations to be solved are:
i) The mass balance on silane:

$$q_f C_{S,f} - q_e C_{S,e} = A_{TL} r_{HT} + A_{TF} r_{HT} + V r_{HD} \qquad (11)$$

ii) The mass balance on silicon vapor:

$$0 - q_e C_{Si,e} + V r_{HD} = V r_{HN} + A_{TL} r_{DL} + A_{TF} r_{DF} \qquad (12)$$

iii) The balance on fines given by eqs. (8-9):
iv) The energy balance which can be shown to readily simplify to the following equation for temperature:

$$T_e = \frac{h_D A_D / h_w A_w}{1 + h_D A_D / h_w A_w} T_D + \frac{1}{1 + h_D A_D / h_w A_w} T_w \qquad (13)$$

v) The growth rate of large seed particles

$$\frac{dR_L}{dt} = \frac{M_{Si}}{\rho_{Si}} \frac{(r_{HT} + r_{DL})}{\phi_s} + \frac{m_{Sca}}{4 \pi R_L^2 N_L \rho_{Si}} \qquad (14)$$

The total surface area of large and small particles A_{TL}, A_{TF}, respectively, are estimated from their average size.

A computer program was developed for solution of eqs. (11-14) and eqs. (8-9). In addition to the quantities already discussed many parameters of the fluidized bed such as bed height at minimum fluidization, the elutriation constant, heat transfer coefficients, etc. are estimated from the literature [7,20, 21]. It should be noted that the distributor must be cooled to keep its temperature below 350° to prevent silane CVD in the nozzles. When the distributor and wall temperatures are known bed temperature is given by eq. (13). When bed temperature is known eq. (13) is bypassed in the program.

The required input variables for the CSTR model are bed diameter, initial weight of solids, initial size of solids, gas flow rate, inlet gas temperature, inlet gas composition and pressure. Equations (8-9), (11) and (12) are solved for the initial seed size and the RHS of eq. (14) is then evaluated. The process is repeated for various selected values of seed size. This generates the set of pairs of values of R_L vs dR_L/dt which is numerically integrated to establish the relationship between time and particle (seed) radius. It should be noted that the CSTR as presented here has no adjustable parameters. Given the input quantities, the rate forms and transport properties are calculated by the appropriate subroutines and reactor performance is predicted, i.e. the growth rate of seeds, amounts of fines elutriated and silane conversion are calculated.

The fraction of silane that ended in the form of free fines, F_f, is calculated at each set of conditions from

$$F_f = 1 - \frac{\text{growth rate of large particles}}{\text{total rate of silane deposition}} = 1 - \frac{A_{TL}(r_{HT} + r_{DL})M_{Si} + m_{Sca}}{(A_{TL} r_{HT} + A_{TF} r_{HT} + V r_{HD})M_{Si}} \qquad (15)$$

172

Bubbling Fluidized Bed (FBBR) Model

A large diameter fluidized bed of silicon particles operated at three to ten times the minimum fluidization velocity will behave like a bubbling bed provided bed diameter is large enough. However, since the information regarding the kinetics of the system under study is not very refined, a sophisticated bubbling bed model is not necessary. Only the key features of the bubbling bed need to be incorporated in the model. These are the existence of three distinct regions: the grid region, emulsion region (including the cloud) and the bubble region. We assume that in beds of large particles jets form in the grid region. We assume gas to be in plug flow in the jets, and jet penetration height is calculated from the Yang and Keairns' [22] formulas. When jets break up, gas is assumed to pass through the emulsion phase at minimum fluidization velocity. There are no gradients between gas and particles in the emulsion phase which is assumed well mixed. The excess gas, $u-u_{mf}$, forms bubbles which rise in plug flow. Average bubble diameter, average bubble volume fraction, bubble rise velocity, etc. are calcualted from the available correlations. The overall mass and heat transfer coefficients between bubbles and emulsion are evaluated based on the approach suggested by Kunii and Levenspiel [7]. The mass and heat transfer exchange coefficients between jets and emulsion are calculated as a multiple of bubble-emulsion exchange coefficients as suggested by Weimer and Clough [23]. This multiplicative factor f_{jb} defined by

$$K_{je} = f_{jb} \, (K_{be})_b \tag{16}$$

is the only adjustable parameter for the bubbling bed model. It is also assumed that no large particles are present in the jets and bubbles.

The schematic of the bubbling bed model is shown in Figure 2. The various pathways described in Figure 1 can take place now in each of the three regions: jets, bubbles and emulsion. In addition, one must account for the interchange between the various regions. The equations for the mass balance on silane, silicon vapor and fines and for the energy balance in each of the three regions are lengthy and will be omitted here but are given elsewhere [24].

The input parameters besides those required by the CSTR model include the specification of the distributor, i.e. number or orifice holes, hole diameter, etc. The details of the computer algorithm are reported elsewhere [24]. Given all input parameters the program calculates silane conversion, fraction of silane in form of fines and growth rate of large particles. Repeated calculations at various particle sizes lead to desired time on stream-particle size relationship.
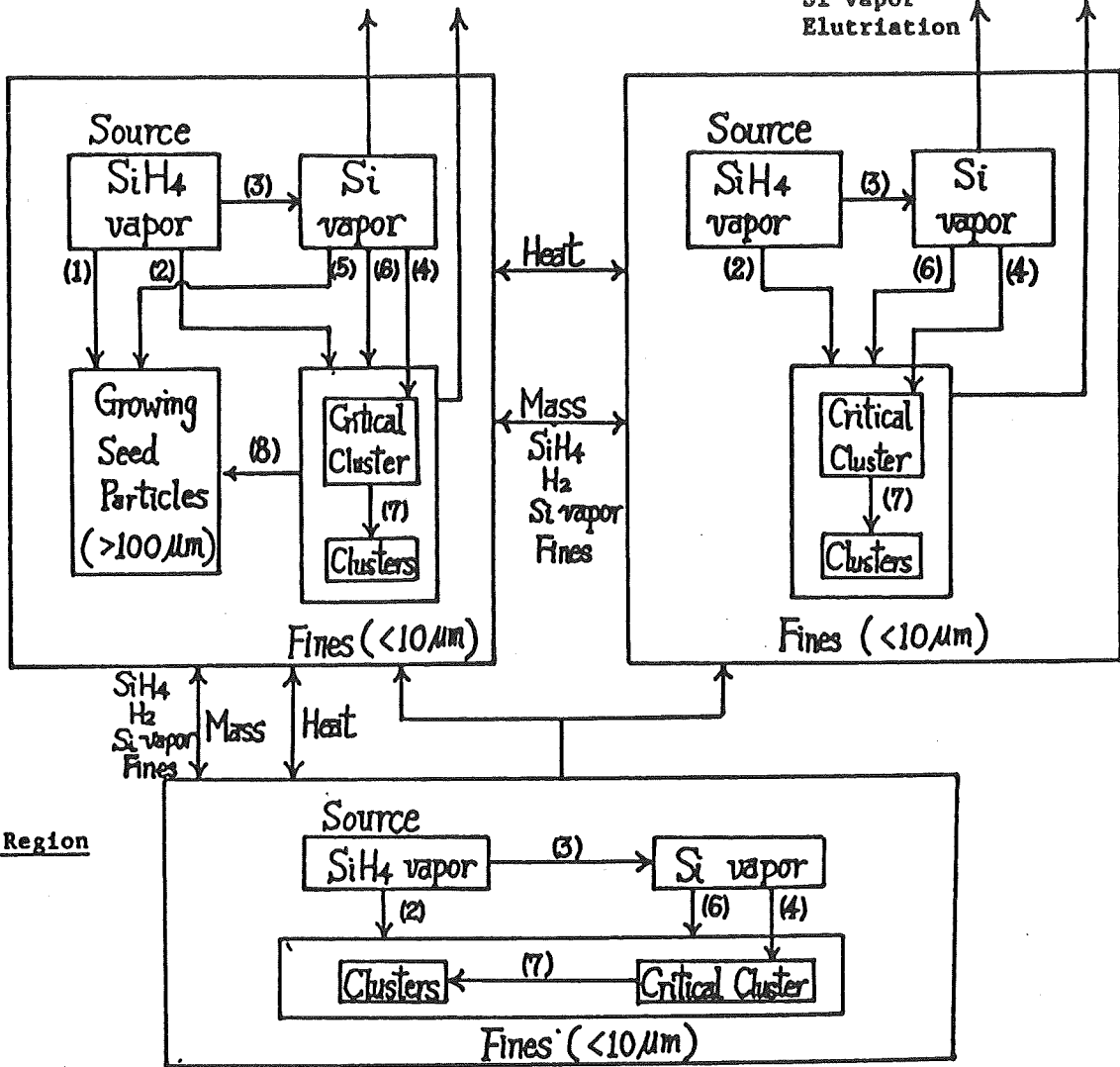

RESULTS AND DISCUSSION

Model predicted results are compared with two JPL experimental runs in Table 1. Both models predict reasonably well the production rate and final particle size. However, model discrimination is impossible because the experimental runs were of insufficient duration so that the actual final particle size could not be determined accurately. This also leads to problems in the mass balance for the experimental runs and slight discrepancies in reported production rates and final particle size.

III. **Emulsion Phase**   Si vapor   Fines   II. **Bubbling Region**   Fines
Elutriation Elutriation   Elutriation

Source

SiH₄ vapor   (3)   Si vapor

(1) (2)   (5) (6) (4)   Heat

Growing Seed Particles (>100 μm)   (8)   Critical Cluster   (7)   Clusters

Mass SiH₄ H₂ Si vapor Fines

Fines (<10 μm)

Source

SiH₄ vapor   (3)   Si vapor

(2)   (6) (4)

Critical Cluster   (7)   Clusters

Fines (<10 μm)

Si vapor Elutriation

SiH₄ H₂ Si vapor Fines   Mass   Heat

I. **Grid Region**

Source

SiH₄ vapor   (3)   Si vapor

(2)   (6) (4)

Clusters   (7)   Critical Cluster

Fines (<10 μm)

(1) CVD Growth on seed particles
(2) CVD growth on fines
(3) Homogeneous SiH₄ decomposition
(4) Homogeneous nucleation
(5) Brownian diffusion of Si Vapor
     into seed particles

(6) Molecular bombardment of
     Si vapor to fines
(7) Coagulation of fines
(8) Scavenging of fines by seed particles

Figure 2.   Schematic of the Fluidized Bubbling Bed Reactor (FBBR)
            Model for Silane Pyrolysis.

Table 1. Comparison of the CSTR and FBBR Model Predictions and Experimental Results for Two JPL Runs

Silicon Seed		Experimental Conditions			
Weight (Kg)	$\bar{d}_p$ (μm)	Silane Feed Conc. (%)	Bed temp. (°C)	Total gas flow rate (moles/min)	Duration (min)
10.50	227	20	650	3.0	90
11.34	212	80	650	2.5	173

PRODUCT COMPARISON

Experimental Data		Model Predicted (CSTR)		Model Predicted (FBBR)	
Production rate	$\bar{d}_p$ (μm)	Production rate (Kg/hr)	$\bar{d}_p$ (μm)	Production rate	$\bar{d}$ (μm)
0.87	235.5	1.00	237.4	0.93	236.6
3.50	241.5	3.30	260.3	3.16	257.7

Reactor Specifications: Bed diameter 15.4 cm (6.065" I.D.); Number of orifice holes in distributor: 4,500.

Orifice area: 0.02 cm^2; Distributor temperature: 200°C; Entering gas temperature: 200°C.

In order to illustrate the dominant pathways in silane conversion to silicon the modeling results for the two runs of Table 1 are presented schematically in Figure 3 for the CSTR model. It is clear that in an ideal CSTR gas-solid contacting is very efficient, micromixing is excellent and homogeneous nucleation and fines formation can be effectively suppressed. For example even at 80% SiH_4 in the feed (Figure 3b) 84% of decomposed silane (2.82 kg/h) reacts by CVD on the growing seed particles, 15% (0.49 kg/h) decomposes homogeneously and 1% (0.035 kg/h) reacts by CVD on the fines. Silane conversion is over 99%. The Si vapor is formed at a rate of 0.49 kg/h, but 75% of it (0.36 kg/h) is effectively scavenged by diffusion to and condensation on seed particles, while only 25% (0.12 kg/h) contributes to the mass generation of fines. The nucleation rate is kept at a very low level of 4 x 10^{-5} kg/h. The nucleated fines gain 78% of their mass (0.12 kg/h) by molecular bombardment of silicon vapor and 22% (0.035 kg/h) by CVD of silane on fines. Most importantly due to excellent contacting 70% (0.11 kg/h) of the fines formed are scavenged by large particles and only 30% (0.04 kg/h) are elutriated. This means that in an ideal CSTR at 650°C bed temperature and at a high production rate of 3.3 kg/h only 1.5% of silane would end in the undesirable form of fines at the reactor exit even at 80% SiH_4 in the feed.

Figure 4 illustrates the FBBR model predictions for the JPL run listed as example 1 in Table 1 at 20% SiH_4 in the feed. The values computed in Figure 4 are based on the assumption that the exchange between jets and emulsion is fifty times faster than between bubbles and emulsion, i.e. f_{jb} = 50. Homogeneous decomposition is favored over CVD on seeds in the jet region due to poor gas-
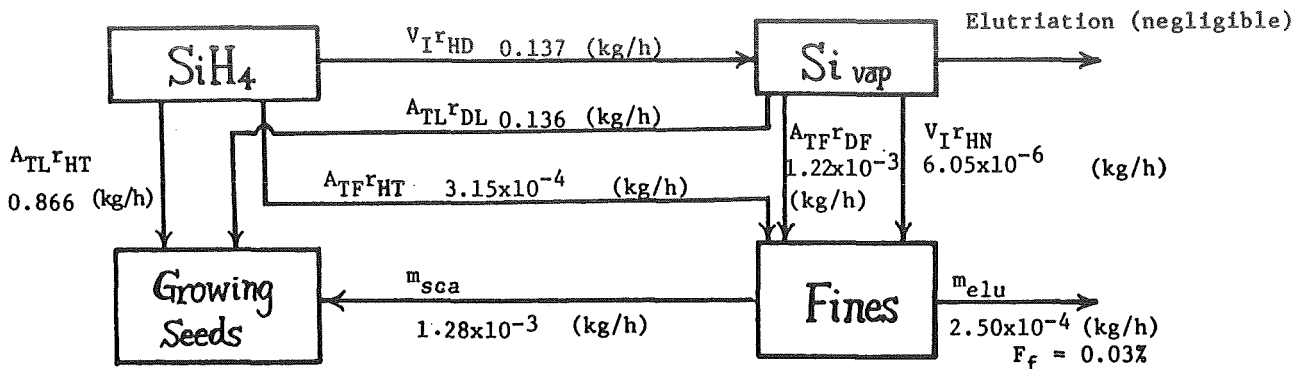
Figure 3a.   Net growth rate: 1.00 (kg/h)
                 Backmixed (CSTR) Reactor: 20% SiH_4 in the Feed
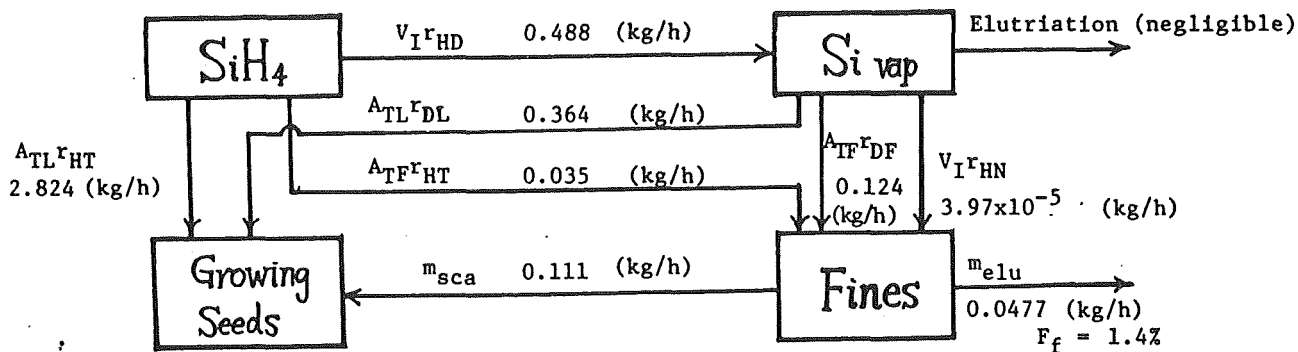

Figure 3b.   Net growth rate: 3.30 (kg/h)
                 Backmixed (CSTR) Reactor: 80% SiH_4 in the Feed

Figure 3.   Rates of Various Pathways for Silane Decomposition
               as Calculated by the CSTR Model for Bed Temperature
               of 650°C

      3a.   20% SiH_4 in the feed
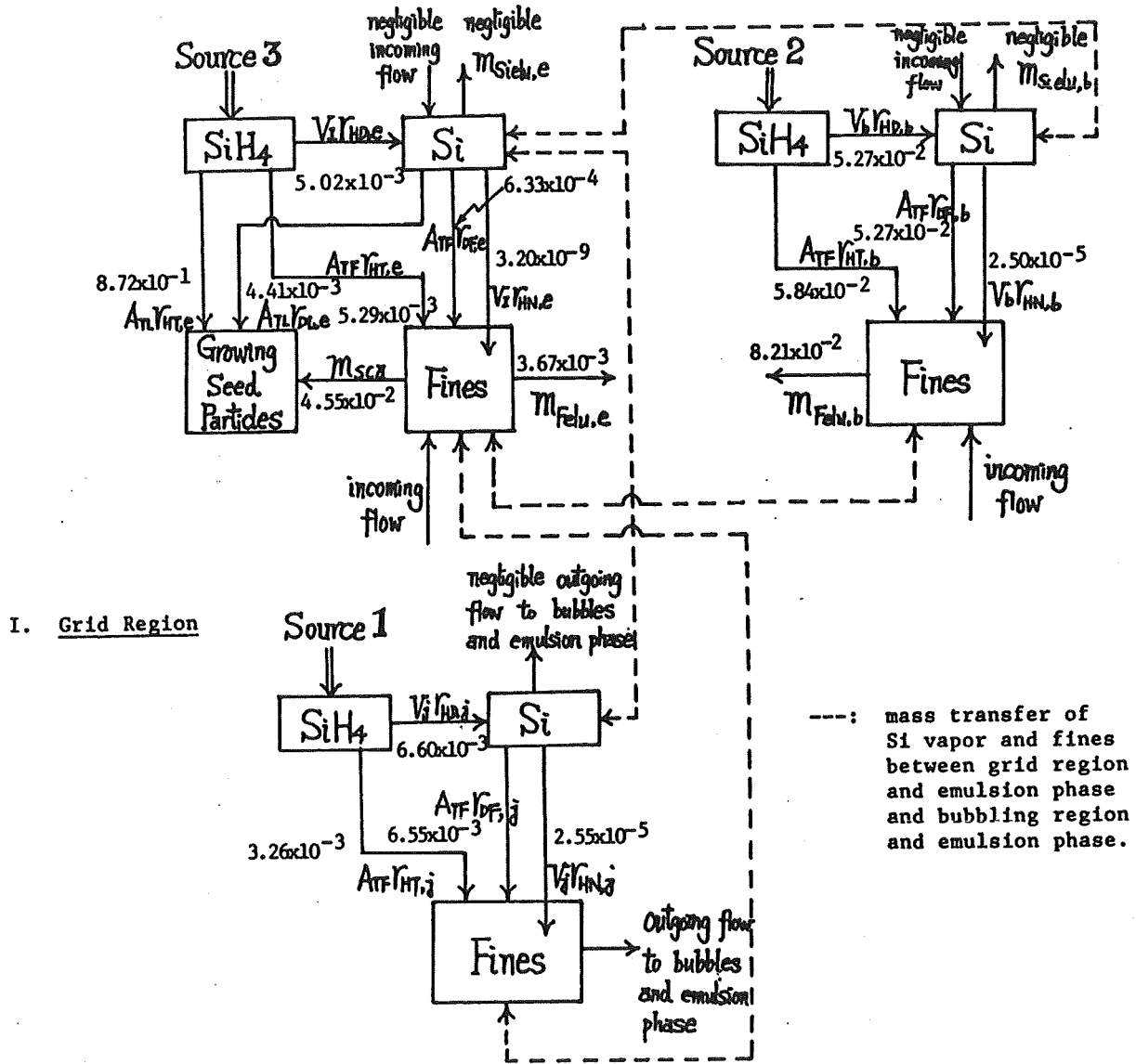
      3b.   80% SiH_4 in the feed

176

Figure 4.   Rates of Various Pathways for Silane Decomposition as
            Calculated by the FBBR Model (Run 1, T_e = 650°C,
            f_{jb} = 50).

solid contacting in spite of the high exchange coefficients. Most of the homogeneous nucleation takes place in the jets (grid region) (2.6×10^{-5} kg/h) followed up by nucleation in the bubbles (2.5×10^{-5} kg/h) while little occurs in the emulsion phase (3.2×10^{-9} kg/h). The fines gain the most mass in the bubbles at a rate of 0.11 kg/h, followed by the grid region with the rate of 0.010 kg/h and the emulsion region with the rate of 0.0059 kg/h. Bubbles are the main culprit in formation of fines since 88% of the mass of fines is generated there. The predicted fraction of silane that is elutriated as silicon fines is 8.1% which exceeds the experimental value of 3%. However, in the run of such short duration the mass balance is difficult to close and it is questionable whether all the fines have been detected in the experimental run. There are reasons to believe that actual elutriation rate of fines is higher than reported values.

The comparison of CSTR and FBBR (f_{jb} = 50) predictions for deposition rate with 20% SiH_4 in the feed and as a function of bed temperature and gas flow rate is illustrated in Figure 5. At low bed temperatures and at low gas flow rate (i.e. close to minimum fluidization conditions) CSTR and FBBR predictions are close. While mathematically this is to be expected, it is doutbful that CSTR behavior can be achieved in practice since solids circulation would not be vigorous enough at close to minimum fluidization conditions. It is clear that the CSTR model gives an upper bound on deposition rate as argued earlier. At higher temperatures FBBR predictions can deviate significantly from CSTR behavior due to increased production of fines. This is to be expected for two reasons. The homogeneous decomposition has a higher activation energy than the CVD reaction and is favored at higher temperatures. At the same time bubble expansion is more drastic at higher temperatures and the gas bypassing problem is aggravated.

A limited parametric sensitivity study of the model was performed. The changes in deposition rate, silane conversion and formation of fines were determined as a function of the following quantities: (i) the kinetic form for homogeneous decomposition [11,12,13], (ii) the jet-emulsion exchange coefficient, i.e. variation in f_{jb} values, (iii) grid design, (iv) method of treatment of the population balance. It was shown [24] that the variations in the kinetic forms and method of treatment of the population balance for fines have a limited effect on production rate and fines elutriation. The model is, however, most sensitive to the jet-emulsion exchange coefficient. Table 2 illustrates that an increase in the jet-emulsion exchange coefficient in the limit leads to CSTR behavior. Unfortunately, there is no reliable model for the grid region based on which the exchange coefficients could be tied initimately to grid design. Therefore, two different assumptions are made in order to estimate the effects of grid design on reactor performance. In the first case, it is assumed that jet emulsion exchange is governed mainly by bed dynamics which is primarily affected by bed diameter, height and total gas flow. the ratio of jet-emulsion and bubble-emulsion exchange was set a f_{jb} = 50 for all grids. The effect of grid design is illustrated in Table 3. Clearly, silane overall conversion is hardly affected by grid design. Higher deposition rates (and lower formation and elutriation of fines) are obtained at lower jet velocities. Higher jet penetration at the same gas velocity also favors improved deposition rate. Yang and Keairns [22] indicate that the jet penetration length is proportional to $d_o^{0.8} u_o^{0.36}$ where d_o is orifice
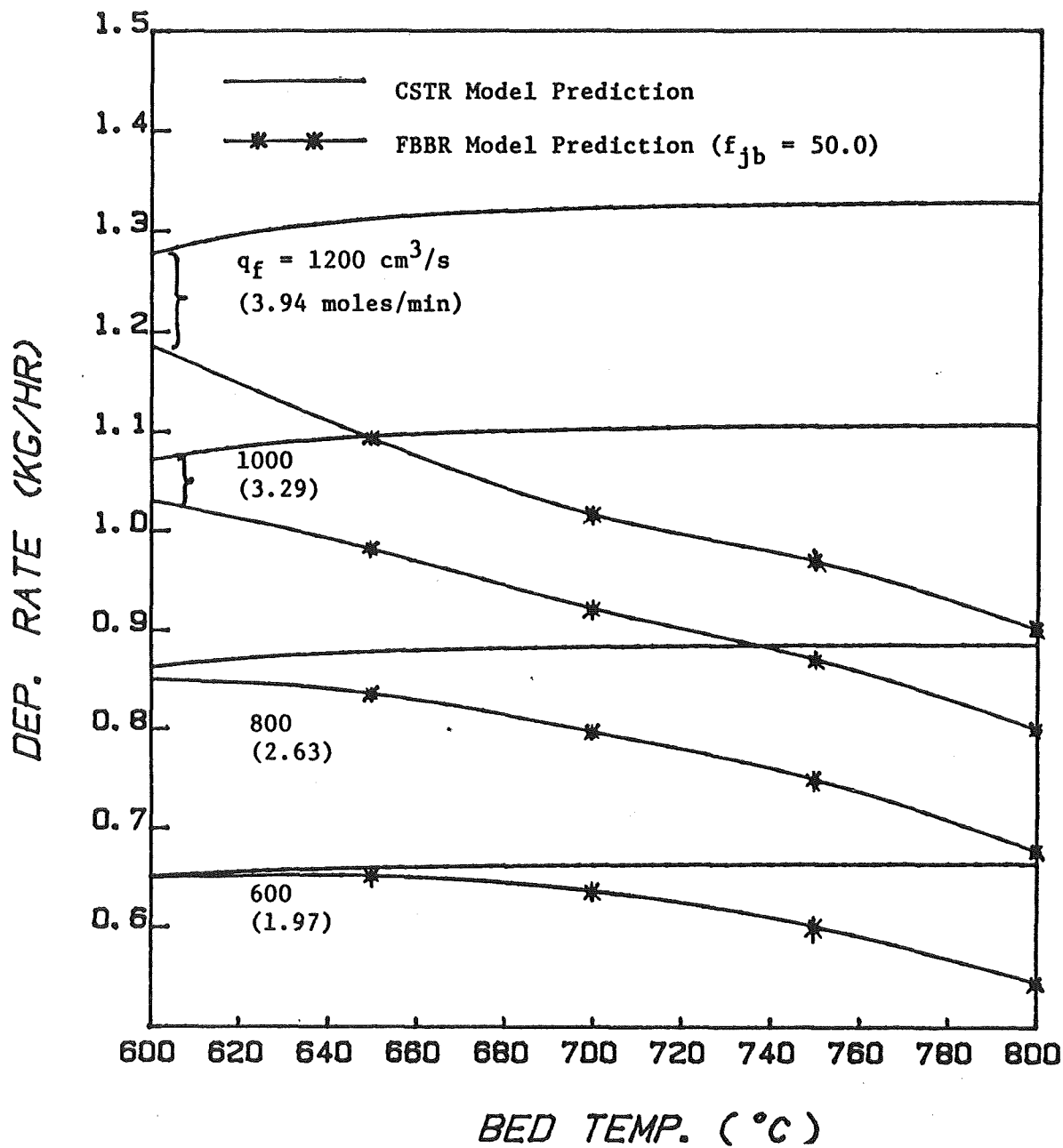
Figure 5. Comparison of CSTR and FBBR Model Predictions for
Deposition Rate (Run 1).

Table 2. Comparison of the FBBR Model at Different Levels of Jet-Emulsion Exchange and the CSTR Model (Conditions of Run 1, Table1.)

	FBBR			CSTR
	$f_{jb} = 10$	$f_{jb} = 50$	$f_{jb} = 100$	--
Silane Conversion (%)	99.50	99.21	99.15	99.04
Fines Elutriation (%)	30.9	9.1	1.6	0.0
Deposition Rate (kg/h)	0.696	0.922	0.986	1.002

Table 3. Effect of Grid Design (Constant $f_{jb} = 50$)

	Grid 1	Grid 2	Grid 3	Grid 4	Grid 5
	$A_{ro}=0.002cm^2$ $N_t=4,500$	$A_{ro}=0.02cm^2$ $N_t=450$	$A_{ro}=0.02cm^2$ $N_t=45$	$A_{ro}=0.2cm^2$ $N_t=45$	$A_{ro}=2.0cm^2$ $N_t=45$
Jetting height(cm)	0.35	0.83	1.97	2.12	2.29
Jetting velocity (cm/s)	10.1-29.5	101-256	1014-1680	101-284	10.1-34.3
Silane Conversion (%)	99.2	99.5	99.7	99.3	99.3
Fines Elutriation (%)	8.1	30.7	47.8	21.0	0.9
Deposition Rate (kg/h)	0.92	0.70	0.53	0.79	1.00
$N_t^{0.64}A_{ro}(cm^2)$	4.4	1.0	0.23	2.3	23

diameter and u_o is the velocity at the orifice. At fixed total gas flow rate it can then be shown that the gas residence time in the jetting region is proportional to $N_t^{0.64}d_o^{2.08} = N_t^{0.64}A_{ro}$ where N_t is the total number of orifice holes and A_{ro} is the surface area of an individual orifice. Last row of Table 3 gives the value of this group for each grid. It is apparent that deposition rate correlates at least qualitatively with the residence time in the jetting region.

On the other hand one can assume that the jet-emulsion exchange is dominated by the grid hydrodynamics and that f_{jb} increases proportionately with jet velocity. The deposition rate for grids 2, 3 and 4 which now have f_{jb} = 150, 450, 150, respectively, is increased compared to values in Table 3, but not sufficiently to approach the superior performance of grid 5. However, grid 4 would yield now a deposition rate of 0.97 (kg/h) and fines elutriation of 3.1% which is better than the grid 1 performance. This indicates, as expected, that $N_t^{0.064}A_{ro}$ is not the only measure of grid performance. The exchange coefficient is another key variable. Its a priori predictions at present are not possible. Grid 5 design is also unrealistic.

The above results indicate the importance of grid design and gas-solids contacting in the grid region on reactor performance. Good jet penetration, high gas residence time in the jetting region and excellent jet-emulsion

exchange are necessary for suppression of formation of fines. The current models for the grid region are insufficient to fully quantify reactor performance and can benefit from further improvements. It should be noted that the current FBBR model is capable of predicting temperature gradients in the grid region and that such gradients have been observed experimentally.

CONCLUSIONS

An ideal backmixed reactor model (CSTR) and a fluidized-bed bubbling reactor model (FBBR) have been developed for silane pyrolysis. Silane decomposition is assumed to occur via two pathways: homogeneous decomposition and heterogeneous CVD. Both models account for homogeneous and heterogeneous silane decomposition, homogeneous nucleation, coagulation and growth by diffusion of fines, scavenging of fines by large particles, elutriation of fines and CVD growth of large seed particles. At present the models do not account for attrition.

The preliminary comparison of model predictions with JPL experimental results shows reasonable agreement. The CSTR model with no adjustable parameter yields a lower bound on fines formed and upper estimate on production rate. The FBBR model overpredicts the formation of fines but could be matched to experimental data by adjusting the unknown jet-emulsion exchange coefficients. In the limit of low gas flow-rate and large exchange coefficients the FBBR model is reduced to the CSTR model provided the jet region becomes negligibly small.

The models indicate clearly that in order to suppress formation of fines (smoke) one must achieve good gas-solid contacting in the grid region and eliminate or suppress the formation of bubbles.

ACKNOWLEDGEMENT

NOMENCLATURE

A_D	- area of the distributor excluding orifice holes, cm^2
A_{TF}	- total surface area of fines in the reactor, cm^2
A_{TL}	- total surface area of seed particles in the reactor, cm^2
A_w	- area of vessel wall, cm^2
C_{SiH_4}	- concentration of SiH_4, mol/cm^3
$C_{S,f}, C_{S,e}$	- concentration of SiH_4 in the feed fas and in the backmixed reactor, respectively, mol/cm^3
$C_{Si,e}, C_{Si}$	- concentration of Si vapor, mol/cm^3
C_{Sio}	- equilibrium Si vapor concentration, mol/cm^3
C_{Si}^*	- the supersaturated concentration of silicon in the gas phase from homogeneous decomposition, mol/cm^3
d_{PL}	- diameter of seed particle, cm

$\bar{d}_{PL}, \bar{d}_{PF}$ – average diameter of seed particles and fines, respectively, cm

D – particle diffusion coefficient, cm^2/s

E – single seed particle collection efficiency, Eq. (13)

f_{jb} – ratio relating jetting-emulsion intercharge to bubble-emulsion interchange

F_f – fraction of silane decomposed into fines

h_D – heat transfer coefficient between bed and distributor, $J/cm^2 sK$

h_w – heat transfer coefficient between bed and surface, $J/cm^2 sK$

k – Boltzman constant, 1.38066×10^{-23} J/molecule K

K_{je} – interchange coefficient between jets and emulsion per unit volume of jets, s^{-1}

$(K_{be})_b$ – interchange coefficient between bubbles and emulsion phase based on volume of bubbles, s^{-1}

m – mass of molecule, g/molecule

m_{Sca} – total amount of fines captured by seed particles, g/s

M_0 – total number of particles per unit volume of gas, cm^{-3}

M_1 – total volume of particles per unit volume of gas, cm^3/cm^3

M_{Si} – molecular weight of silicon, g/mol

$n_v(v,t)$ – size distribution density function of fines per unit volume of fluid, $cm^{+3}cm^{+3}$

N_A – Avogadro's number, 6.02×10^{23} molecules/mol

N_L – total number of seed particles in the reactor

Pe – Peclet number

P_{Si} – partial pressure of Si vapor, atm

P_{Si}° – equilibrium Si vapor pressure, atm

q_e – volumetric flow rate of gas in the backmixed reactor, cm^2/s

q_f – inlet volumetric flow rate of gas, cm^3/s

r^* – radius of the critical nucleus, cm

r_{DF} – rate of molecular bombardment of Si vapor on fines, $mol/cm^2 s$

r_{DL} – rate of molecular diffusion of Si vapor to seed particles, $mol/cm^2 s$

r_{DH} – rate of homogeneous decomposition of SiH_4, $mol/cm^3 s$

r_{HN} – rate of homogeneous nucleation, $mol/cm^3 s$

r_{HT} – rate of heterogeneous CVD of SiH_4, $mol/cm^2 s$

R_g – gas constant, 8.31441 J/mol K

R_L – radius of seed particles, cm

$R_G(v)$ – rate of fine particle growth from heterogeneous CVD growth and Si molecular bombardment, cm^3/s

S – supersaturation ratio, P_{Si}/P_{Si}°

t – time scale, s

T, T_e – temperature of the interstitial gas, K

T_D – temperature of distributor, K

T_w – temperature of vessel wall, K

u_{mf} – superficial fluid velocity at minimum fluidizing conditions, cm/s

v, v_F – volume of fine particles, cm^3

v_L – volume of seed particles, cm^3

v^* – critical volume of fine generated from homogeneous nucleation, cm^3

V_I – total volume of interstitial gas, cm^3

Greek Symbols

α_c — condensation coefficient

$\alpha\ (v, v_L)$ — scavenging coefficient, s^{-1}

$\beta\ (v, \tilde{v}), \beta_0$ — coagulation coefficient, cm^3/s

$\delta\ (v-v*)$ — Delta function, cm^{-3}

ε_{mf} — void fraction in a bed at minimum fluidizing conditions

μ — viscosity of gas, $g/cm\ s$

ρ_{Si} — density of silicon, g/cm^3

σ — rate constant of fine particle growth, cm/s

$\bar{\sigma}$ — specific surface free energy, J/cm^2

ϕ_s — sphericity of a particle

REFERENCES

1. Dudukovíc, M. P., "Reactor Models for CVD of Silicon", The Science of Silicon Material Preparation Workshop, Phoenix, Arizona, August 1982, JPL Publication 83-13, 199-226 (1983).
2. Hsu, G., R. Hogle, N. Rohatgi and A. Morrison, "Fines in Fluidized Bed Silane Pyrolysis", J. Electrochem. Society 131 (3), 660 (1984).
3. Rohatgi, N. and G. Hsu, "silicon Production in a Fluidized Bed Reactor: A Parametric Study", JPL Report No. 5101-129, October (1983).
4. Grace, J. R., "An Evaluation of Models for Fluidized-Bed Reactors", AIChE Symp. Series 67 No. 116, 159-167 (1971).
5. Grace, J. R., "Generalized Models for Isothermal Fluidized Bed Reactors", Recent Advances in the Engineering Analysis of Chemically Reacting Systems, (Doraiswamy, L. K., ed.) Ch. 13, Wiley Eastern, New Delhi (1984).
6. Yates, J. G., Fundamentals of Fluidized Bed Chemical Processes, Butterworths, London (1983).
7. Kunii, D. and O. Levenspiel, Fluidization Engineering, Wiley, New York (1969).
8. Fane, A. G. and C. Y. Wen, "Fluidized Bed Reactors", Handbook of Multiphase Systems (Hetsroni, G., ed.), Hemisphere, Washington, D.C. (1983).
9. Coltrin, M. E., R. L. Kee, and J. A. Miller, "A Mathematical Model of the Coupled Fluid Mechanics and Chemical Kinetics in a Chemical Vapor Deposition Reactor", J. Electrochem. Soc., 131(2), 425 (1984).
10. Neudorfl, P., Jodhan, A. and O. P. Strausz, "Mechanism of the Thermal Decomposition of Monosilane", J. Phys. Chem., 84(3), 328 (1980).
11. Hogness, T. R., T. L. Wilson and W. C. Johnson, J. Am. Chem. Soc., 58, 108 (1936).
12. Purnell, J. H. and Walsh, R., Proc. Royal Soc., London, 293, 543-561 (1966).
13. Ring, M. A. and O'Neal, H. E., "Kinetics and Mechanism of Silane Decomposition", Proceedings of the Flat Plate Solar Array Project Workshop on the Science of Silicon Material Preparation, DOE/JPL-1012-81, pp. 63-75 (1983).
14. Iya, S. K. Flagella, R. N. and F. S. DiPaolo, "Heterogeneous Decomposition of Silane in a Fixed Bed Reactor", J. Electrochem. Soc. 129(7), 1531 (1982).
15. Abraham, F. F., Homogeneous Nucleation Theory, Academic Press, N.Y. (1974).

16. Hinds, W. C., <u>Aerosol Technology: Properties, Behavior, and Measurement of Airborne Particles</u>, Wiley, N.Y. (1982).
17. Friedlander, S. K., <u>Smoke, Dust and Haze: Fundamentals of Aerosol Behavior</u>, Wiley, N.Y., (1977).
18. Doganoglu, Y., V. Jog, K. V. Thambimuthu, and R. Clift, "Removal of Fine Particulates From Gases in Fluidized Beds", Trans. I. Chem. E., Vol. 56, pp. 239-248 (1978).
19. Peters, M. H., L. S. Fan, and T. L. Sweeney, "Simulation of Particulate Removal in Gas-Solid Fluidized Beds", AIChE J., Vol. 28, No. 1, pp. 39-49 (1982).
20. Wen, C. Y. and R. F. Hashinger, "Elutriation of Solid Particles From a Dense Phase Fluidized Bed", AIChE J., 6, 220 (1960).
21. Wender, L. and G. T. Cooper, "Heat Transfer Between Fluidized-solids Beds and Boundary Surfaces", AIChE J., 4, 15 (1958).
22. Yang, W. C. and D. L. Keairns, "Estimating the Jet Penetration Depth of Multiple Vertical Grid Jets", I&EC Fundamentals, 18, 317 (1979).
23. Weimer, A. W. and D. E. Clough, "The Influence of Jetting-Emulsion Mass and Heat Interchange in A Fluidized Bed Coal Gasifier", AIChE Symp. Series 205 (No. 77), 51 (1981).
24. Dudukovic, M. P. Ramachandran, P. A., and S. Lai, "Modeling of Fluidized-Bed Reactors for Manufacture of Silicon from Silane", JPL Final Technical Report, DOE/JPL-956737-85/7, September 30, 1985.

C-3

DISCUSSION

LORD: Have you looked at the characteristics of an ideal grid design for suppressing fines?

DUDUKOVIC: No.

LORD: Can you give any indications of the direction which you should go, based on your model?

DUDUKOVIC: Well, I am hesitant to speculate on that, because grid design was not part of my expertise when we started on this project. Now, after we have finished the study, we are convinced that it has a determining effect. First, we would like to crystallize our ideas as to how we should do an experimental study. Since it is very difficult for us to run a silicon system, we would use a mock system to determine the exchange coefficiencies and then, when we are sure that we are on the right path, we could go further.

FLAGAN: Is it true that you neglected the diffusional resistance between the gas and the large particles that were growing?

DUDUKOVIC: That is correct. The diffusional resistance is small compared to the chemical vapor deposition growth rate, and so the major resistance (i.e., the rate limiting step) is growth by chemical vapor deposition.

FLAGAN: Is that true throughout the entire range of conditions that you've looked at?

DUDUKOVIC: It seems that way.